Journal of Solid State Chemistry **167,** 274–281 (2002)
doi:10.1006/jssc.2002.9530

Open-Framework Rubidium Halides Incorporated in Cadmium Oxalate Host Lattices

R. Vaidhyanathan, Srinivasan Natarajan, and C. N. R. Rao[1]

Chemistry and Physics of Materials Unit, Jawaharlal Nehru Centre for Advanced Scientific Research, Jakkur, P.O. Bangalore 560 064, India

Received October 29, 2001; in revised form January 22, 2002, accepted February 1, 2002; published online March 22, 2002

DEDICATED TO PROFESSOR GALEN D. STUCKY ON THE OCCASION OF HIS 65TH BIRTHDAY

The metathetic reaction between $CdBr_2$ and rubidium oxalate under hydrothermal conditions yields [RbBr] $[Cd_6(C_2O_4)_6]\cdot 2H_2O$, I, containing Cd_6O_{24} clusters with the Br^- ions in the center. The RbBr moiety forms a three-dimensional F*m*3*m* structure, but with a unit cell double that of the normal stable phase. The hydrothermal reaction between rubidium oxalate and $CdCl_2$ in the presence of NO_3^- ions gives $[Rb_2Cd(NO_3)(Cl)(C_2O_4)(H_2O)]$, II, containing cadmium chloro-oxalate layers. The Rb^+ ions present between the layers interact with the Cl atoms to form a one-dimensional RbCl chain decorated by NO_3^- groups.

INTRODUCTION

Size-selective incorporation of ions in molecular cavities or channels constitutes an important aspect of molecular recognition and supramolecular host–guest chemistry (1–5). We have recently shown that expanded structures of alkali halides can be incorporated in the host lattice of cadmium oxalate. Thus, a compound of the formula [KC1] $[Cd_6(C_2O_4)_6]\cdot 2H_2O$ has been isolated, where a three-dimensional KC1 structure with double the unit cell of ordinary KC1 occurs in the cadmium oxalate host (6). Such a host–guest system is indeed unique. What is remarkable is that these unusual hybrid compounds are formed by a simple metathetic reaction between $CdCl_2$ and an alkali oxalate. We have extended our studies to explore whether we can indeed obtain other novel alkali halide structures by this method. This is of particular interest since the expanded alkali halide structure can be considered to constitute a new class of open-framework inorganic structures. Our efforts have indeed been successful and we have isolated two new cadmium oxalates $[RbBr][Cd_6(C_2O_4)_6]\cdot 2H_2O$, **I** and $[Rb_2Cd(NO_3)(Cl)(C_2O_4)(H_2O)]$, **II**, containing rubidium halides with novel structures. In this paper, we describe a new rubidium bromide with an expanded three-dimensional structure (**I**), the unit cell parameter being double that of the ordinary RbBr with the rock-salt structure, and a one-dimensional RbCl with a chain structure (**II**).

[1]To whom correspondence should be addressed. E-mail cnrrao@jncasr.ac.in.

EXPERIMENTAL

Synthesis and Initial Characterization

The alkali halide incorporated cadmium oxalates, $[RbBr][Cd_6(C_2O_4)_6]\cdot 2H_2O$, **I**, and $[Rb_2Cd(NO_3)(Cl)(C_2O_4)(H_2O)]$, **II**, were synthesized by metathetic reaction employing hydrothermal methods. For the synthesis of **I**, 0.0424 g of rubidium carbonate was dissolved in a mixture of 1 mL water + 2 mL *n*-butanol. To this 0.093 g of oxalic acid and 0.04 mL acetic acid were added under continuous stirring. Contents were stirred for 20 min, followed by an addition of 0.1 g of $CdBr_2\cdot 4H_2O$. The final mixture with the composition, $CdBr_2\cdot 4H_2O : 0.63Rb_2CO_3 : 2.54H_2C_2O_4 : 2.41CH_3COOH : 75n\text{-}C_4H_9OH : 63H_2O$, was homogenized at room temperature, sealed in a 23 mL PTFE stainless-steel autoclave and heated at 150°C for 78 h. The resulting product, a crop of cube-like crystals were filtered, washed with deionized water and dried at ambient conditions. For the synthesis of **II**, a mixture of the composition, $0.8CdCl_2 : 0.2Cd(NO_3)_2 : 1.5Rb_2CO_3 : 2.0H_2C_2O_4 : 1.5CH_3COOH : 33\ n\text{-}C_4H_9OH : 33H_2O$ was reacted at 150°C for 78 h resulting in a crop of rod-like crystals. The role of acetic acid in the synthesis of **I** and **II** is still not clear, the absence of which does not yield desired products. X-ray diffraction (XRD) patterns of the powdered crystals of **I** and **II** indicated that the products were new materials; the patterns were entirely consistent with the structures determined by single-crystal X-ray diffraction. Further characterizations were carried out by IR spectroscopy and thermogravimetric analysis (TGA) studies.

0022-4596/02 $35.00

TABLE 1
Crystal Data and Structure Refinement Parameters for I, $Cd_6(C_2O_4)_6 \cdot RbBr \cdot H_2O$ and II, $[Rb_2Cd(Cl)(NO_3)(C_2O_4)(H_2O)]$

Parameters	$Cd_6(C_2O_4)_6 \cdot RbBr \cdot H_2O$	$Rb_2(Cl)(NO_3)Cd(C_2O_4)(H_2O)$
Empirical formula	$H_4C_{12}O_{26}Cd_6BrRb$	$H_2C_2O_8NCdClRb_2$
Crystal system	Trigonal	Orthorhombic
Space group	*R*-3 (no. 148)	*Pbca* (no. 56)
Crystal size (mm)	$0.07 \times 0.07 \times 0.07$	$0.04 \times 0.06 \times 0.06$
a (Å)	9.4141(2)	12.0600(10)
b (Å)	9.4141(2)	10.7599(2)
c (Å)	23.9946 (5)	15.7905(10)
α (°)	90°	90°
β (°)	90°	90°
γ (°)	120°	90°
Volume (Å^3)	1841.63(10)	2049.04(4)
Z	6	8
Formula mass	1403.85	482.84
ρ_{calc} (g cm^{-3})	3.787	3.130
λ (Mo$K\alpha$) Å	0.71073	0.71073
μ (mm^{-1})	8.823	11.850
θ range (°)	2.55–23.20	2.58–23.28
Total data collected	2602	8062
Unique data	591	1473
Observed data ($I > 2\sigma(I)$)	579	1278
R_{int}	0.0421	0.0476
R indexes [$I > 2\sigma(I)$]	$R_1 = 0.0381$,[a] $wR_2 = 0.0972$[b]	$R_1 = 0.0261$,[a] $wR_2 = 0.0644$[b]
R (all data)	$R_1 = 0.0387$, $wR_2 = 0.0977$	$R_1 = 0.0321$, $wR_2 = 0.0665$
Goodness of fit	1.144	1.123
No. of variables	71	138
Largest difference map Peak and hole (eÅ^{-3})	0.694 and −4.306	0.836 and −0.625

[a] $R_1 = \sum||F_o| - |F_c||/\sum|F_o|$.
[b] $wR_2 = \{\sum[w(F_o^2 - F_c^2)^2]/\sum[w(F_o^2)^2]\}^{1/2}$, $w = 1/[\sigma^2(F_o)^2 + (aP)^2 + bP]$, $P = [\max.(F_o^2, 0) + 2(F_c)^2]/3$, where $a = 0.0412$ and $b = 155.4846$ for **I** and $a = 0.0332$ and $b = 0.4837$ for **II**.

Single-Crystal Structure Determination

A suitable single crystal of each compound was carefully selected under a polarizing microscope and glued at the tip of a thin glass fiber with cyano-acrylate (super glue) adhesive. Single-crystal structure determination by X-ray diffraction was performed on a Siemens Smart-CCD diffractometer equipped with a normal focus, 2.4 kW sealed tube X-ray source (Mo$K\alpha$ radiation, $\lambda = 0.71073$ Å) operating at 50 kV and 40 mA. A hemisphere of intensity data was collected at room temperature in 1321 frames with ω scans (width of 0.30° and exposure time of 20 s per frame) in the 2θ range 5.0–46.5°. Pertinent experimental details for the structure determinations are presented in Table 1.

The structures were solved and refined by using SHELXTL-PLUS (7) suite of program. The hydrogen positions for the water molecules in **I** and **II** could not be located in the difference Fourier Maps. The last cycles of refinement included atomic positions for all the atoms and anisotropic thermal parameters for all the atoms. Full-matrix-least-squares structure refinement against $|F^2|$ was carried out using SHELXTL-PLUS package of programs (7). Details of the final refinements are given in Table 1. The final atomic coordinates, selected bond distances and angles for compound **I** are presented in Tables 2 and 3, for **II** in Tables 4 and 5.

TABLE 2
Final Atomic Coordinates [$\times 10^4$] and Equivalent Isotropic Displacement Parameters [Å$^2 \times 10^3$] for I, $[RbBr][Cd_6(C_2O_4)_6] \cdot 2H_2O$

Atom	*x*	*y*	*Z*	U_{eq}[a]
Cd(1)	2558(1)	3845(1)	962(1)	10(1)
Rb(1)	0	0	0	14(1)
Br(1)	3333	6667	1667	35(1)
C(1)	4444(12)	4143(12)	−135(4)	12(2)
C(2)	−920(12)	1822(13)	1479(4)	11(2)
O(1)	1110(9)	4999(9)	584(3)	14(2)
O(2)	3146(9)	3173(9)	94(3)	16(2)
O(3)	472(8)	2949(8)	1637(3)	13(2)
O(4)	2190(9)	1187(9)	1051(3)	17(2)
O(100)	6667	3333	762(20)	246(30)

[a] U_{eq} is defined as one-third trace of the orthogonalized tensor U_{ij}.

TABLE 3
Selected Bond Distances and Bond Angles for I, $[RbBr][Cd_6(C_2O_4)_6]\cdot 2H_2O$

Atom	Distance (Å)	Atom	Distance (Å)
Cd(1)–O(1)	2.310(7)	Rb(1)–O(4)#3	3.091(7)
Cd(1)–O(2)	2.323(7)	Rb(1)–O(4)#7	3.091(7)
Cd(1)–O(3)#1	2.350(7)	Rb(1)–O(4)#5	3.091(7)
Cd(1)–O(3)	2.352(7)	Cd(1)–Br(1)#1	2.917(7)
Cd(1)–O(4)	2.358(7)	Cd(1)–Br(1)#8	2.917(7)
Cd(1)–O(1)#2	2.399(7)	Cd(1)–Br(1)#9	2.917(7)
Rb(1)–O(2)#3	2.983(7)	Cd(1)–Br(1)#8	2.917(7)
Rb(1)–O(2)#4	2.983(7)	Cd(1)–Br(1)#2	2.917(7)
Rb(1)–O(2)	2.983(7)	Cd(1)–Br(1)	2.917(7)
Rb(1)–O(2)#5	2.983(7)	C(1)–O(2)	1.230(13)
Rb(1)–O(2)#6	2.983(7)	C(1)–O(1)#3	1.272(13)
Rb(1)–O(2)#7	2.983(7)	C(2)–O(4)#4	1.233(13)
Rb(1)–O(4)#6	3.091(7)	C(2)–O(3)	1.264(13)
Rb(1)–O(4)#4	3.091(7)	C(1)–C(1)#10	1.56(2)
Rb(1)–O(4)	3.091(7)	C(2)–C(2)#11	1.57(2)
Moiety	**Angle (°)**	**Moiety**	**Angle (°)**
O(1)–Cd(1)–O(2)	93.1(3)	O(3)#1–Cd(1)–O(1)#2	87.3(2)
O(1)–Cd(1)–O(3)#1	147.7(2)	O(3)–Cd(1)–O(1)#2	146.7(2)
O(2)–Cd(1)–O(3)#1	114.9(3)	O(4)–Cd(1)–O(1)#2	123.0(3)
O(1)–Cd(1)–O(3)	81.7(3)	O(4)#4–C(2)–O(3)	125.2(9)
O(2)–Cd(1)–O(3)	142.2(2)	O(2)–C(1)–O(1)#3	126.0(9)
O(3)#1–Cd(1)–O(3)	85.01(8)	O(2)–C(1)–C(1)#10	119.1(12)
O(1)–Cd(1)–O(4)	136.6(3)	O(1)#3–C(1)–C(1)#10	114.9(11)
O(2)–Cd(1)–O(4)	73.8(2)	O(4)#4–C(2)–C(2)#11	118.5(11)
O(3)#1–Cd(1)–O(4)	70.5(2)	O(3)–C(2)–C(2)#11	116.2(11)
O(3)–Cd(1)–O(4)	84.5(3)	O(5)–N(1)–O(6)	119.9(5)
O(1)–Cd(1)–O(1)#2	87.8(4)	O(5)–N(1)–O(7)	119.6(5)
O(2)–Cd(1)–O(1)#2	69.5(2)	O(6)–N(1)–O(7)	120.5(5)

Note. Symmetry transformations used to generate equivalent atoms: #1: $x-y+\frac{2}{3}, x+\frac{1}{3}, -z+\frac{1}{3}$; #2: $-y+1, x-y+1, z$; #3: $y, -x+y, -z$; #4: $-y, x-y, z$; #5: $-x, -y, -z$; #6: $-x+y, -x, z$; #7: $x-y, x, -z$; #8: $-x+\frac{2}{3}, -y+\frac{4}{3}, -z+\frac{1}{3}$; #9: $y-\frac{1}{3}, -x+y+\frac{1}{3}$; #10: $y-\frac{1}{3}, -x+y+\frac{1}{3}, -z+\frac{1}{3}$; #11: $-x+1, -y+1, z$; #12: $-x-\frac{1}{3}, -y+\frac{1}{3}, -z+\frac{1}{3}$.

RESULTS

The asymmetric unit of $[RbBr][Cd_6(C_2O_4)_6]\cdot 2H_2O$, **I**, consists of 10 non-hydrogen atoms, of which seven atoms belong to the cadmium oxalate framework and the remaining are the rubidium, bromide and water. The Cd atoms in **I** are six-coordinated with respect to oxygen atoms forming a D_{3h} trigonal prism. The connectivity between the Cd and the oxalate oxygens results in a cadmium oxide octahedral cluster of the composition $[Cd_6O_{24}]$. The clusters are further linked into a three-dimensional framework by the oxalate units. The Br^- ions occupy the center of this octahedral $[Cd_6O_{24}]$ cluster (see inset in Fig. 1), with the charge compensating Rb^+ ion residing outside, in the cavities formed by the linkage between the clusters and the oxalate units (Fig. 1). The important feature of the structure of **I** is the arrangement of the Rb^+ and Br^- ions. The Rb^+ and Br^- ions are arranged such that they form a perfectly ordered three-dimensional rock-salt ($Fm3m$) structure with interpenetrating fcc lattices (Fig. 2). The unit cell length of the RbBr in **I** is 13.496 Å, which is nearly double that of the ordinary RbBr with the rock-salt structure (6.855 Å), as shown in Fig. 2.

The Cd–O distances in **I** are in the range 2.310(7)–2.399(7) Å (av. Cd–O = 2.355 Å). The O–Cd–O angles are in the range 69.5(2)–147.4(2)° (av. O–Cd–O = 102.9) (Table 3). The C–O bond distances are in the range 1.230(13)–1.272(13) Å (av. 1.251 Å), and the average O–C–O bond angles have a value of 125.6°. The average Cd–Br distance is 2.917 Å. The Rb atoms are 10-coordinated with respect to oxygen atoms with an average Rb–O distance of 3.026 Å. All the oxygen atoms interacting with rubidium are at distances < 3.1 Å, which is the upper limit for significant $M \ldots O$ interaction (M = Na, K, Rb, etc.) (8). Selected bond distances and angles in **I** are presented in Table 3.

The asymmetric unit of $[Rb_2Cd(NO_3)(Cl)(C_2O_4)(H_2O)]$, **II**, contains 15 non-hydrogen atoms. The Cd atom is coordinated to four oxalate oxygens, one terminal water and a chlorine atom, forming a distorted octahedron (Fig. 3). The framework of **II** is made up of cadmium and oxalate units linked to form layers in the *ab*-plane. The Cl^- ions and the water molecule bound to the cadmium protrude into the inter-layer space (Fig. 3). The connectivity between the oxalate and the cadmium atoms results in a six-membered aperture within the layers. Such layers get stacked along the *c*-axis and the Rb^+ ions and the NO_3^- ions occupy the inter-lamellar spaces and interact with the Cl^- ions and

TABLE 4
Final Atomic Coordinates [$\times 10^4$] and Equivalent Isotropic Displacement Parameters [$Å^2 \times 10^3$] for I, $[RbBr][Cd_6(C_2O_4)_6]\cdot 2H_2O$

Atom	x	y	z	U_{eq}[a]
Cd(1)	692(1)	1568(1)	7410(1)	16(1)
Rb(1)	−1433(1)	−464(1)	6139(1)	27(1)
Rb(2)	3296(1)	−348(1)	6214(1)	30(1)
Cl(1)	823(1)	1452(2)	5826(1)	36(1)
C(1)	−1019(4)	3735(5)	7402(3)	15(1)
C(2)	3279(4)	2538(5)	7595(3)	15(1)
O(1)	1543(3)	−265(4)	7617(2)	22(1)
O(2)	2264(3)	2687(3)	7601(2)	21(1)
O(3)	−1223(3)	1507(3)	7433(2)	19(1)
O(4)	24(3)	3642(3)	7444(2)	22(1)
O(100)	470(3)	1550(4)	8894(2)	36(1)
N(1)	−1796(4)	2438(5)	4987(3)	28(1)
O(5)	−1385(4)	2128(4)	4305(3)	44(1)
O(6)	−1602(4)	3481(4)	5281(3)	47(1)
O(7)	−2428(3)	1703(4)	5368(3)	43(1)

[a] U_{eq} is defined as one-third trace of the orthogonalized tensor U_{ij}.

TABLE 5
Selected Bond Distances of II, $[Rb_2Cd(Cl)(NO_3)(C_2O_4)(H_2O)]$

Atom	Distance (Å)	Atom	Distance (Å)
Cd(1)–O(1)	2.248(4)	Rb(2)–O(3)#3	2.981(3)
Cd(1)–O(2)	2.266(4)	Rb(2)–O(4)#1	3.010(4)
Cd(1)–O(3)	2.311(4)	Rb(2)–O(5)#6	3.107(4)
Cd(1)–O(4)	2.372(4)	Rb(2)–O(6)#11	3.102(5)
Cd(1)–O(100)	2.359(4)	Rb(1)–Cl(1)#6	3.361(2)
Cd(1)–Cl(1)	2.510(2)	Rb(1)–Cl(1)	3.449(2)
Rb(1)–O(2)#2	2.986(4)	Rb(2)–Cl(1)	3.609(2)
Rb(1)–O(7)	2.892(4)	Rb(2)–C(1)#5	3.645(5)
Rb(1)–O(3)	2.955(4)	Rb(2)–Cl(1)#1	3.656(2)
Rb(1)–O(6)#4	2.956(5)	C(1)–O(1)#2	1.248(7)
Rb(1)–O(4)#5	2.969(3)	C(1)–O(4)	1.263(6)
Rb(1)–O(2)#5	2.986(4)	C(2)–O(2)	1.234(6)
Rb(1)–O(4)#2	2.970(3)	C(2)–O(3)#3	1.263(6)
Rb(1)–O(6)#10	2.956(5)	C(1)–C(2)#3	1.541(8)
Rb(2)–O(3)#7	2.981(3)	C(2)–C(1)#7	1.541(8)
Rb(2)–O(4)#8	3.010(4)	N(1)–O(5)	1.231(6)
Rb(2)–O(1)	3.063(4)	N(1)–O(6)	1.237(5)
Rb(2)–O(7)#6	3.076(5)	N(1)–O(7)	1.253(6)
Rb(2)–O(6)#9	3.102(5)		
Atom	**Angle (°)**	**Atom**	**Angle (°)**
O(1)–Cd(1)–O(2)	93.69(13)	O(3)–Cd(1)–Cl(1)	94.40(9)
O(1)–Cd(1)–O(3)	115.42(13)	O(4)–Cd(1)–Cl(1)	95.20(9)
O(2)–Cd(1)–O(3)	148.17(13)	O(100)–Cd(1)–Cl(1)	175.57(12)
O(1)–Cd(1)–O(100)	84.26(13)	O(2)–C(2)–O(3)#7	125.8(5)
O(2)–Cd(1)–O(100)	88.13(13)	O(1)#2–C(1)–O(4)	125.1(5)
O(3)–Cd(1)–O(100)	82.60(13)	O(1)#2–C(1)–C(2)#3	116.2(5)
O(1)–Cd(1)–O(4)	167.71(12)	O(4)–C(1)–C(2)#3	118.7(5)
O(2)–Cd(1)–O(4)	77.39(13)	O(2)–C(2)–C(1)#7	115.9(5)
O(3)–Cd(1)–O(4)	71.78(12)	O(3)#7–C(2)–C(1)#7	118.3(5)
O(100)–Cd(1)–O(4)	86.97(13)	O(5)–N(1)–O(6)	119.9(5)
O(1)–Cd(1)–Cl(1)	94.14(10)	O(5)–N(1)–O(7)	119.6(5)
O(2)–Cd(1)–Cl(1)	96.11(9)	O(6)–N(1)–O(7)	120.5(5)

Note. Symmetry transformations used to generate equivalent atoms: #1: $-x+\frac{1}{2}, y+\frac{1}{2}, z$; #2: $-x, y+\frac{1}{2}, -z+\frac{3}{2}$; #3: $x-\frac{1}{2}, y, -z+\frac{3}{2}$; #4: $-x, y-\frac{1}{2}, -z+\frac{3}{2}$; #5: $-x, -y, -z+1$; #6: $-x-\frac{1}{2}, y-\frac{1}{2}, z$; #7: $x-\frac{1}{2}, -y-\frac{1}{2}, -z+1$; #8: $x+\frac{1}{2}, y, -z+\frac{3}{2}$; #9: $x+\frac{1}{2}, -y+\frac{1}{2}, -z+1$; #10: $-x+\frac{1}{2}, y-\frac{1}{2}, z$; #11: $x+\frac{1}{2}, -y-\frac{1}{2}, -z+1$; #12: $-x-\frac{1}{2}, y+\frac{1}{2}, z$.

water molecules in the interlayer space (Fig. 4). The adjacent layers are shifted by nearly $\frac{1}{2}$ of the unit cell along the *b*-axis, resulting in a *ABABAB*... type of stacking as shown in Fig. 5. The Rb(1) and Rb(2) atoms appear to be at the center of the six-membered apertures present within the cadmium oxalate layers (Fig. 3). The interaction of the Rb(2) with the Cl^- ions results in a one-dimensional RbCl chain along the *b*-axis. The Rb(1) atom forms a dimer with the Cl^- ions, which are further linked with the Rb(2) forming a layer with 12-membered aperture in the *ab*-plane as shown in Fig. 6a. Alternatively, Rb(1) along with Cl^- ions and NO_3^- ions forms a layer with ten-membered apertures (Fig. 6b). Such layers are reminiscent of Zn phosphate layers observed recently (9). The NO_3^- ions interact with the Rb atoms in both bidendate and monodendate modes within these layers. The Rb(2) on the other hand, forms a capped one-dimensional chain with both Cl^- and NO_3^- ions. Thus, the one-dimensional RbCl chain described here is different from the one-dimensional KBr chains reported earlier (6). The Rb atoms and the NO_3^- ions form a cation excess (Rb_2NO_3) slab (Fig. 7). These slabs get sandwiched between the cadmium chloro-oxalate layers.

The Cd–O distances in **II** are in the range 2.248(4)–2.372(4) Å (av. 2.311 Å) and the Cd–Cl distance is 2.510(2) Å (Table 5). The O–Cd–O angles are in the range 71.8(1)–167.7(1)° (av. O–Cd–O = 101.6°). The Cl atom occupies the apical position making an average O–Cd–Cl angle of 95.0° with the equatorial oxygen atoms and an angle of 175.6° with the apical oxygen (O100). The C–O bond distances are in the range 1.234(6)–1.263(7) Å (av. 1.253 Å), and the average O–C–O bond angle is 125.45°. The extra-framework species in **II** consists of two Rb and a nitrate ions, situated in the inter-lamellar regions. The average N–O bond distance and O–N–O angle in the NO_3

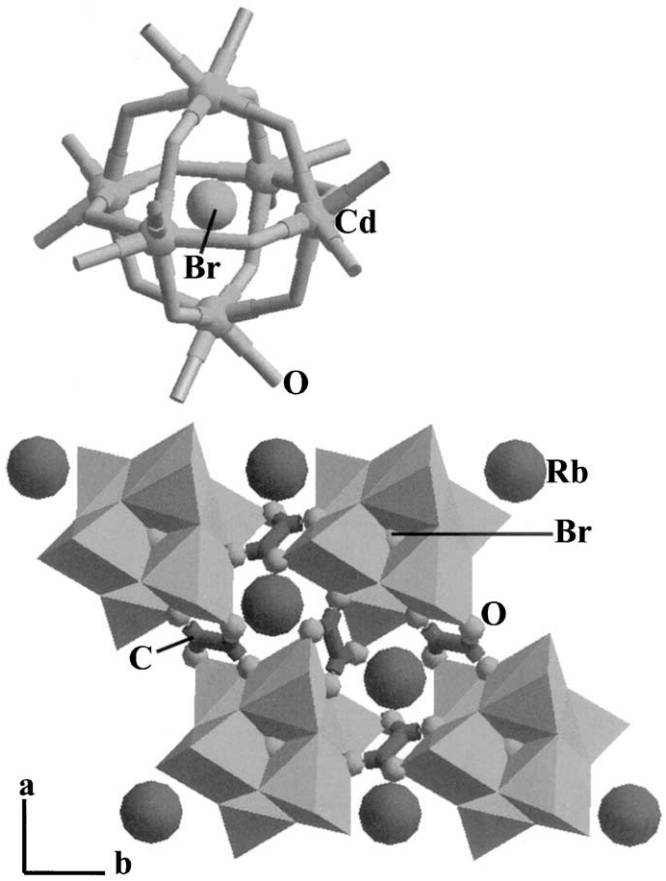

FIG. 1. Structure of $[RbBr][Cd_6(C_2O_4)_6]\cdot 2H_2O$, **I,** in the *ab*-plane, showing the inter-cluster oxalate connectivity. The Rb^+ ions are positioned outside the cluster. Inset shows a single $[Cd_6O_{24}]$ cluster with a Br^- ion at the center.

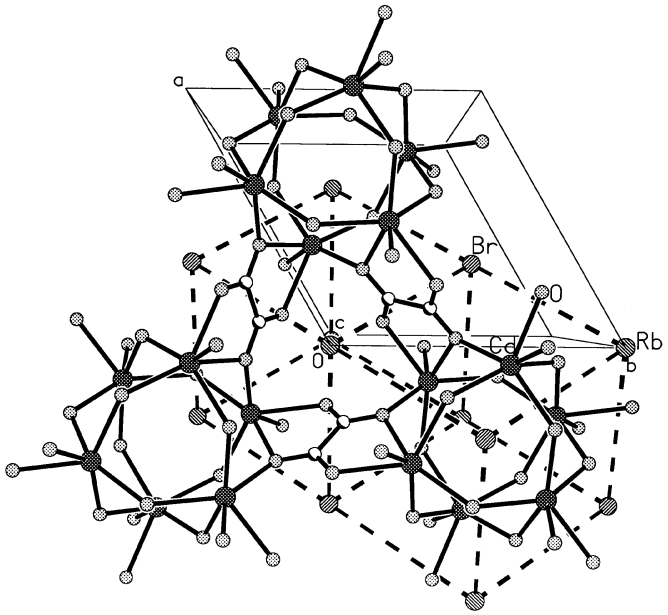

FIG. 2. Structure of **I** showing RbBr in the *Fm3m* structure within the parent cadmium oxalate structure. Note that RbBr is along the [111] direction.

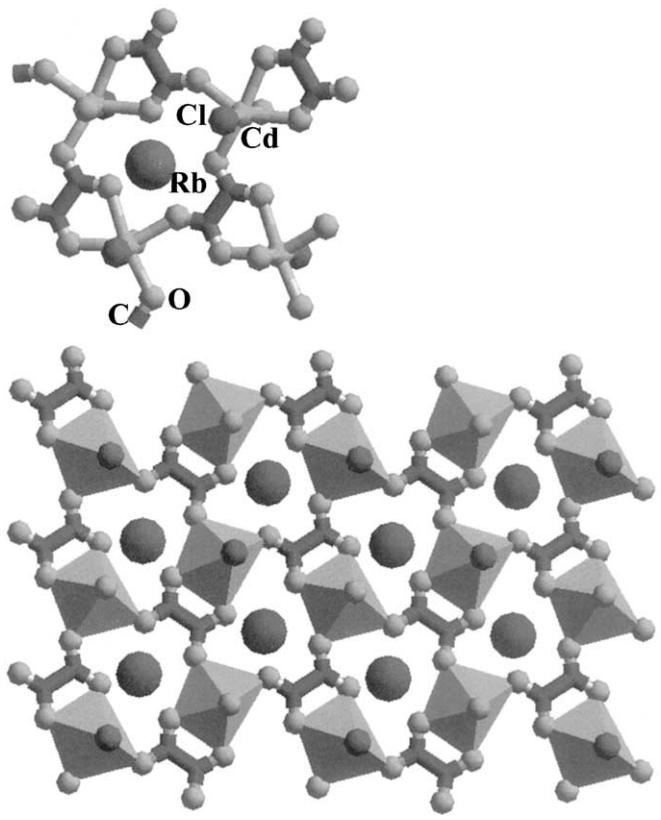

FIG. 3. Structure of $[Rb_2Cd(Cl)(NO_3)(C_2O_4)(H_2O)]$, **II**, in the *ab*-plane showing the layer arrangement. Inset shows the Cl atom and the bound water molecule point into the inter-lamellar space, with the Rb^+ ion located in the six-membered aperture formed by the cadmium oxalate linkages.

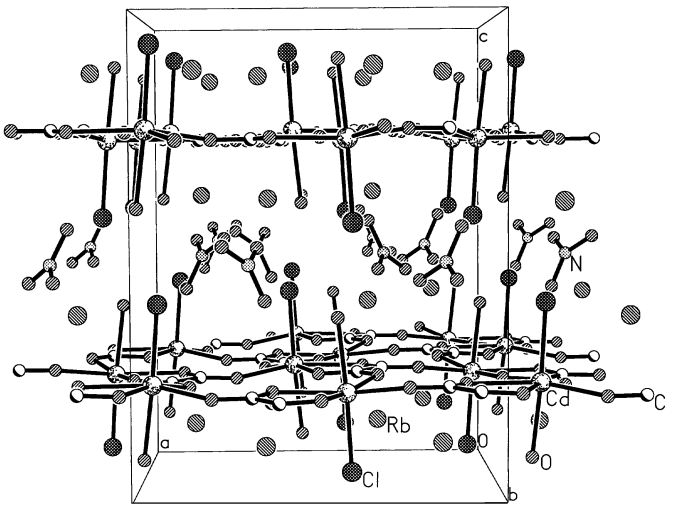

FIG. 4. Layer stacking of $[Rb_2Cd(Cl)(NO_3)(C_2O_4)(H_2O)]$ along the *c*-axis with the Rb^+ ions and the NO_3^- ions occupying the interlayer region. The Cl atoms protrude into the interlayer space.

unit are 1.240 Å and 120, respectively. The two crystallographically distinct Rb atoms are coordinated by 10-[Rb(1)] and 12-[Rb(2)] nearest neighbors. The Rb(1) is surrounded by eight oxygens and two chlorines with average Rb(1)–O and Rb(1)–Cl distances of 2.959 and 3.405 Å, respectively, while the Rb(2) is surrounded by nine oxygens and three chlorines with the average Rb(2)–O and Rb(2)–Cl distances of 3.048 and 3.637 Å, respectively. Selected bond distances and angles in **II** are listed in Table 5.

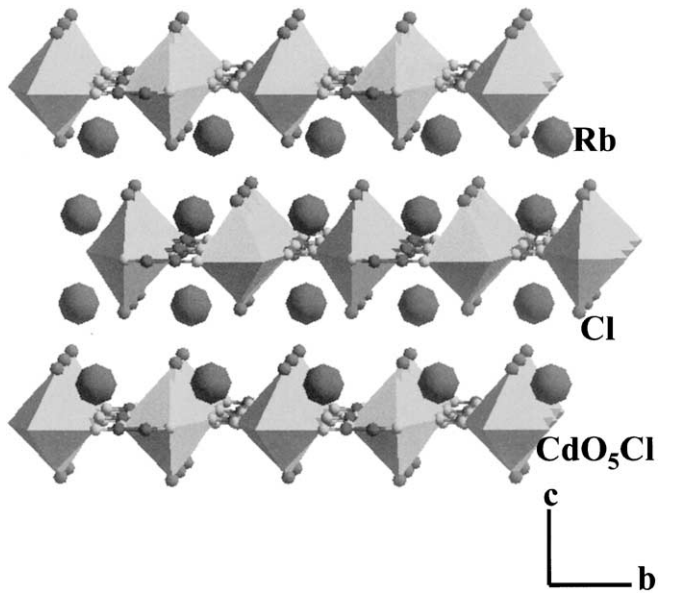

FIG. 5. Polyhedral representation of the cadmium chloro-oxalate layers stacked along the *c*-axis with the Rb^+ ions in the interlayer space. Note the shift in the adjacent layers along the *b*-axis.

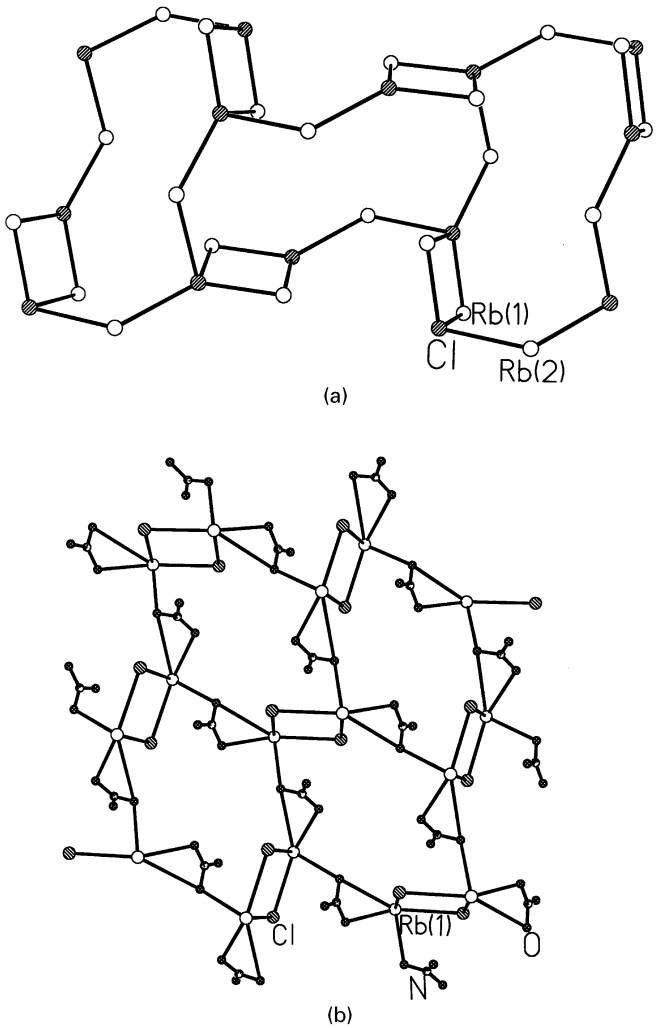

FIG. 6. (a) Layers with 12-membered apertures formed by the Rb atoms and the Cl atoms. (b) Layer formed by the Rb(1), Cl and the NO_3. Note the presence of Rb_2Cl_2 dimers connected by nitrate units.

The infrared spectra of **I** and **II** show characteristic features of the bischelating oxalate (10). The various bands are: ν_{as}(C=O) at 1635(s) cm^{-1} and ν_s (O–C–O) at 1373(m) and 1312(s) cm^{-1}; δ(O–C–O) at 804(s) and 777(s) cm^{-1}, and ν_s(C–C) at 443(s) cm^{-1} for **I**; ν_{as}(C=O) at 1615(s) cm^{-1} and ν_s (O–C–O) at 1364(m) and 1318(s) cm^{-1}; δ(O–C–O) at 805(s) and 776(s) cm^{-1} for **II**. Both **I** and **II** show a broad band around 3500 cm^{-1} due to free water molecules. The ν_s(Cd–O) stretching vibration bands are observed at 512(s) (**I**); 501(s) cm^{-1}(**II**).

Thermogravimetric analysis of compounds **I** and **II** were carried out in O_2 atmosphere (50 ml min^{-1}) in the range 25°–800°C. Whilst **I** showed two distinct mass losses, **II** had three distinct mass losses. In **I**, a gradual mass loss around 100°C followed by a sharp mass loss in the range 350–400°C (43.5%) occurs due to the loss of the extra framework water, oxalate and loss of some CdO (calc. 42.3%). There was a mass loss above 500°C due to the slow evaporation of CdO. In compound **II**, a gradual mass loss occurs in the range 100–160°C due to the bound water molecules; a relatively sharp mass loss occurs in the range 350–450°C due to the loss the oxalate and the decomposition of the rubidium salt. The total mass loss of 24.5% observed for compound **II** is in agreement with the calculated mass loss of 22%. Mass loss above 500°C was observed due to the slow evaporation of CdO.

DISCUSSION

Two new cadmium oxalates incorporating open-framework rubidium halide structures, $[RbBr][Cd_6(C_2O_4)_6]\cdot 2H_2O$, **I**, $[Rb_2Cd(NO_3)(Cl)(C_2O_4)(H_2O)]$, **II**, have been synthesized employing hydrothermal methods. Though a rubidium halide is part of the structure in both **I** and **II**, the manner in which it is arranged within the host oxalate lattice is different. Such differences in the structures are likely to be the result of the hydrothermal conditions employed for the synthesis and the kinetic control of the reaction that operates in such situations.

In **I**, RbBr is present in the cadmium oxalate, while **II** is formed with one unit each of RbCl and $RbNO_3$. RbBr in **I** has a three-dimensional lattice, whilst in **II** one of the Rb atoms, Rb(2), forms a one-dimensional RbCl chain capped on both sides by NO_3^- ions, and Rb(1) forms a Rb_2Cl_2 dimer connected through the nitrate ion forming a layer. Alternatively, the cation excess Rb_2NO_3 slabs in **II** are linked with the Cl atoms to form Rb_2ClNO_3-type layers. A schematic presentation of such an arrangement is shown in Fig. 7. The difference in the structure and dimensionality of the open-framework rubidium halides in **I** and **II** can be attributed to the differences in the structures of the cadmium oxalate host. Accordingly, the three-dimensionally connected

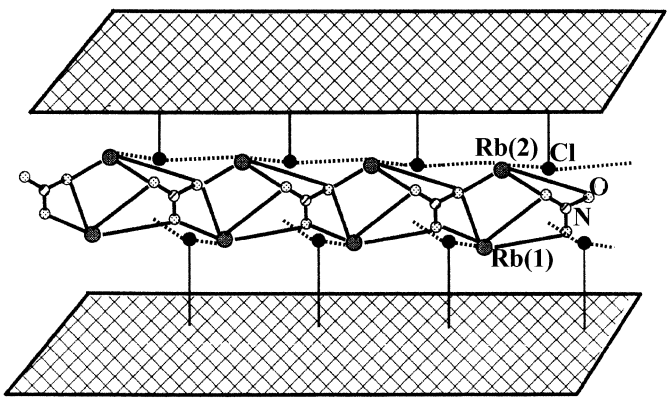

FIG. 7. A schematic representation showing the cation excess Rb_2NO_3 slabs sandwiched between the cadmium chloro-oxalate layers. Note the Cl atoms protruding into the inter-lamellar regions.

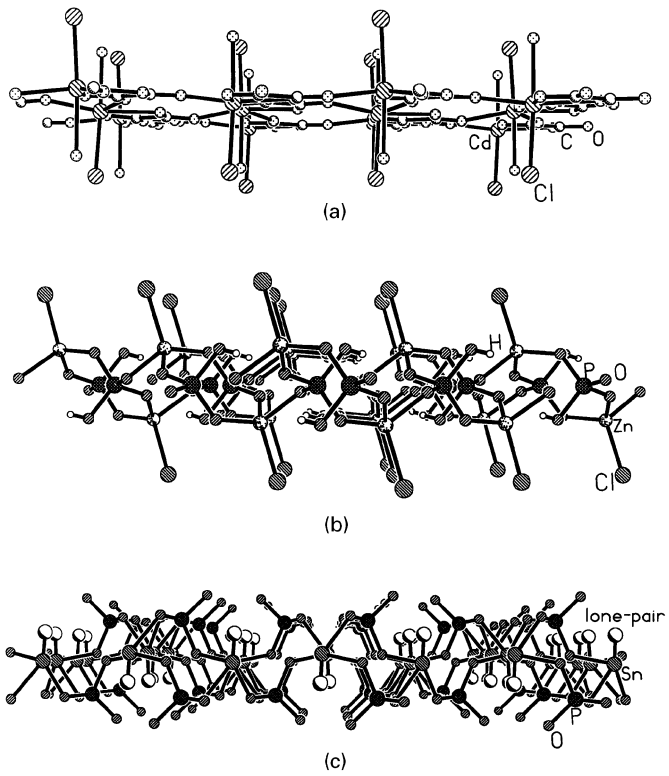

FIG. 8. (a) A single layer of a cadmium chloro-oxalate in $[Rb_2Cd(Cl)(NO_3)(C_2O_4)(H_2O)]$, **II**. (b) A single layer of a zinc chlorophosphate in $[C_6NH_{14}]$ $[ZnCl(HPO_4)]$ (c) A single layer of tin (II) phosphate, in $[C_3N_2H_{12}]_{0.5}$ $[SnPO_4]$. Note the identical positions occupied by the chlorine atoms and the lone pair of Sn^{II}.

cadmium oxalate framework in **I** stabilizes the RbBr lattice with the *Fm*3*m* structure, while the layered cadmium oxalate host in **II** stabilizes the lower-dimensional structure of the guest. Thus, we have an example of host-controlled guest architecture, as against the situation in most open-framework structures where the guest determines the topology of the host (4, 5). The structural parameters of the rubidium halides in **I** and **II** are interesting. In **I**, the Rb–Br distance is 6.748 Å, which is nearly double that of the normal Rb–Br distance in RbBr with the rock-salt structure (Rb–Br = 3.428 Å). In **II**, the average RbCl distance is 3.635 Å, comparable to the distance in normal RbCl (3.291 Å). Thus, RbBr forms an expanded lattice with double the unit-cell length in **I**.

The framework structure of **II** has certain unusual features which merit discussion. The position of the chlorines in **II** provides an interesting comparison with the layered Zn chlorophosphate, $[C_6NH_{14}][ZnCl(HPO_4)]$ (11) and the tin(II) phosphate, $[N_2C_3H_{12}]2[SnPO_4]$ (12). The position of the Cl atoms in the Zn chlorophosphate and the lone pairs in the Sn(II) phosphate are quite similar to those of the chlorines in **II** (Fig. 8). The lone-pair of electrons and chlorine atoms in $[N_2C_3H_{12}]2[SnPO_4]$ and $[C_6NH_{14}]$ $[ZnCl(HPO_4)]$ point in a direction perpendicular to the plane of the layer, with the charge compensating organic amine molecule situated in the inter-lamellar space. In **II**, the chlorine atoms point into the inter-lamellar region occupied by cation excess Rb_2NO_3 slabs (Fig. 4).

The cadmium oxalate hosts in **I** and **II**, themselves make an interesting comparison. Whilst the Cd–O linkages in **I** forms an octahedral cluster of the formula $[Cd_6O_{24}]$, there are no such clusters in **II**. The cluster in **I** is unusual and occurs only in oxalate frameworks (6). Such clusters have, however, been observed in some fluoro compounds of aluminum (13). Thus, in $[(Cp^*AlF)_2SiPh_2]_2$, the molecular core Al_4F_2 is capped by two silicon atoms and forms identical cluster unit, albeit formed by –Al–F–Si–F– network. Whilst $[(Cp^*AlF)_2SiPh_2]_2$ is molecular, **I** has a covalently linked three-dimensional structure, the $[Cd_6O_{24}]$ cluster units being connected through the oxalates. The Cd–O clusters may also be considered to be similar to the Chevrel phases, $A_xMo_6Ch_8$ (A = metal, Ch = S, Se, Te] (14–16). The Chevrel phases contain isolated Mo_6 octahedral clusters encased with S_8 cubes, and the connectivity between such cubes forms tunnels wherein the A-type metal atoms are located.

The loss in Madelung energy of RbBr resulting from the expanded lattice in **I** is compensated by the additional coordination from the oxalate units. The cadmium oxalate framework can be considered to have resulted from the rubidium halide template. There is some similarity between the oxalates under discussion and the metal phosphates of the type $A_2[M_3(X_2O_7)]$[salt] (A = Rb, Cs; M = Mn, Cu; X = P, As) (17). In the latter, the KCl/CsCl structure acts as a structure-directing template. It is interesting that unlike the phosphates, oxides and other materials incorporating metal-anion arrays (18), the cadmium oxalates with RbX (X = Br, Cl) reported here are prepared at considerably milder conditions. It is possible that this method of synthesis can be expanded by using other dicarboxylic acids to form unusual structures of the alkali halides and related compounds. Work on this theme is presently underway.

CONCLUSIONS

Metathetic reactions between cadmium halides and rubidium oxalate carried out under hydrothermal conditions are found to yield novel hybrid host–guest compounds, wherein cadmium oxalates of different structures accommodate novel extended forms of rubidium halides. The dimensionality of the rubidium halide depends on the dimensionality of the Cd oxalate host. This result, in conjection with earlier observations, suggests that such simple hydrothermal reactions provide a means to explore new supramolecular structures with novel properties.

REFERENCES

1. J.-M. Lehn, "Supramolecular Chemistry: Concepts and Perspectives," VCH, New York, 1995.
2. Dalton Discussion No. 3, Inorganic Crystal Engineering, *J. Chem. Soc., Dalton Trans.* **21** (2000).
3. (a) F. Serpaggi and G. Ferey, *Microporous Mesoporous Mater.* **32,** 311 (1999); (b) D. Riou and G. Ferey, *J. Mater. Chem.* **8,** 2733 (1998); (c) C. N. R. Rao, S. Natarajan, A. Choudhury, S. Neeraj, and A. Ayi, *Acc. Chem. Res.* **34,** 80 (2000).
4. (a) C. Livage, C. Egger, M. Nogues, and G. Ferey, *J. Mater. Chem.* **8,** 2743 (1998); (b) C. Livage, C. Egger, and G. Ferey, *Chem. Mater.* **11,** 1546 (1999); (c) R. Kuhlman, G. L. Schemek, and J. W. Kolis, *Inorg. Chem.* **38,** 194 (1999).
5. (a) S. Ayyappan, A. K. Cheetham, S. Natarajan, and C. N. R. Rao, *Chem. Mater.* **10,** 3746 (1998); (b) S. Natarajan, R. Vaidhyanathan, C. N. R. Rao, S. Ayyappan, and A. K. Cheetham, *Chem. Mater.* **11,** 1633 (1999); (c) R. Vaidhyanathan, S. Natarajan, A. K. Cheetham, and C. N. R. Rao, *Chem. Mater.* **11,** 3636 (1999); (d) R. Vaidhyanathan, S. Natarajan, and C. N. R. Rao, *Chem. Mater.* **13,** 3524 (2001).
6. R. Vaidhyanathan, S. Neeraj, P. A. Prasad, S. Natarajan, and C. N. R. Rao, *Angew. Chem. Int. Ed.* **39,** 3470 (2000).
7. G. M. Sheldrick, "SHELXTL-PLUS Program for Crystal Structure Solution and Refinement." University of Göttingen.
8. (a) W. J. Evans, R. Anwander, A. M. Ansari, and J. W. Ziller, *Inorg. Chem.* **34,** 5 (1995); (b) D. L. Clark, J. C. Gordon, J. C. Huffman, R. L. Vincent-Hollis, J. G. Watkin, and B. D. Zwick, *Inorg. Chem.* **33,** 5903 (1994).
9. D. Chidambaram, S. Neeraj, S. Natarajan, and C. N. R. Rao, *J. Solid State Chem.* **147,** 154 (1999).
10. K. Nakamoto, "Infrared and Raman spectroscopy of Inorganic and Coordination Compounds," 5th ed. John Wiley, New York, 1993.
11. S. Neeraj and S. Natarajan, *J. Mater. Chem.* **10,** 1171 (2000).
12. R. Vaidhyanathan and S. Natarajan, *J. Mater. Chem.* **9,** 1807 (1999).
13. B. R. Jagirdar, E. A. Murphy, and H. W. Roesky, *Prog. Inorg. Chem.* **48,** 352 (1999) and references therein.
14. R. Chevrel, M. Sergent, and J. Prigent, *J. Solid State Chem.* **3,** 515 (1971); (b) E. V. Anokhina, M. W. Essig, C. S. Day, and A. Lachgar, *J. Am. Chem. Soc.* **121,** 6827 (1999) and references therein.
15. J. D. Smith and J. D. Corbett, *J. Am. Chem. Soc.* **107,** 5704 (1985).
16. J. D. Corbett, *J. Solid State Chem.* **37,** 335 (1981).
17. Q. Huang, M. Ulutagy, P. A. Michener, and A.-J. Hwu, *J. Am. Chem. Soc.* **121,** 10323 (1999).
18. T. A. Kodenkandath, J. N. Lalena, W. I. Zhou, E. E. Carpenter, Sangregorio, A. U. Falster, J. R. Simmons, C. J. O'Connor, and J. B. Wiley, *J. Am. Chem. Soc.* **121,** 10,743 (1999).